Automated tracking of muscle fascicle orientation in B-mode ultrasound images

Manku Rana [a,*], Ghassan Hamarneh [b], James M. Wakeling [a]

[a] School of Biomedical Physiology and Kinesiology, Simon Fraser University, Burnaby, BC, Canada
[b] Medical Image Analysis Lab, School of Computing Science, Simon Fraser University, Burnaby, BC, Canada

ARTICLE INFO

ABSTRACT

B-mode ultrasound can be used to non-invasively image muscle fascicles during both static and dynamic contractions. Digitizing these muscle fascicles can be a timely and subjective process, and usually studies have used the images to determine the linear fascicle lengths. However, fascicle orientations can vary along each fascicle (curvature) and between fascicles. The purpose of this study was to develop and test two methods for automatically tracking fascicle orientation. Images were initially filtered using a multiscale vessel enhancement (a technique used to enhance tube-like structures), and then fascicle orientations quantified using either the Radon transform or wavelet analysis. Tests on synthetic images showed that these methods could identify fascicular orientation with errors of less than $0.06°$. Manual digitization of muscle fascicles during a dynamic contraction resulted in a standard deviation of angle estimates of $1.41°$ across ten researchers. The Radon transform predicted fascicle orientations that were not significantly different from the manually digitized values, whilst the wavelet analysis resulted in angles that were $1.35°$ less, and reasons for these differences are discussed. The Radon transform can be used to identify the dominant fascicular orientation within an image, and thus used to estimate muscle fascicle lengths. The wavelet analysis additionally provides information on the local fascicle orientations and can be used to quantify fascicle curvatures and regional differences with fascicle orientation across an image.

© 2009 Elsevier Ltd. All rights reserved.

1. Introduction

Muscle architecture, or pennation angle, can be defined as the arrangement of muscle fibers within a muscle relative to the axis of force generation and is one of the main factors that determine the function of a muscle (Lieber and Fridén, 2000). For a given shortening strain of the whole muscle belly, more pennate muscles will tend to undergo smaller strains and strain rates than less pennate fibers. Also, for a given muscle volume, more fibers can be arranged in parallel by increasing the pennation angle; this leads to a greater force production. However, this force is more oblique to the line of action of the muscle belly. Muscles in humans range from nearly parallel fibered, such as the sartorius to highly pennate muscles such as the short head of the biceps femoris with a pennation angle of $23°$. The pennation angle changes during muscle contractions with the fibers rotating to greater pennation angles as the contraction intensity increases. Differences of up to 120–170% in pennation angle between resting and maximally contracted human muscles have been reported (Narici et al, 1996; Herbert and Gandevia 1995). An architectural gear ratio, AGR, has been defined as the ratio of muscle fiber velocity to muscle belly velocity (Azizi et al., 2008) and this changes as the fibers rotate. Changes in the shape of the muscle belly that occur with different muscle forces can cause changes in AGR and rotation and this predisposes the muscle to favor high force–low velocity contractions or high velocity–low force contractions (Azizi et al., 2008). Being able to quantify muscle architecture during dynamic contractions is an important part of determining the function of the muscle.

Muscle fascicle architecture can be quantified non-invasively using diagnostic ultrasound for both isometric situations (Ito et al., 1998; Kawakami et al., 1998; Maganaris et al., 1998; Fukunaga et al., 1997a, b; Blazevich et al., 2006) and during dynamic contractions (Ishikawa et al., 2003; Kurokawa et al., 2001, 2003; Kawakami et al., 2002; Muraoka et al., 2001; Ichinose et al., 2000; Wakeling et al., 2006). Typically, the fascicles have been digitized manually in a process that is both time-consuming and subjective. Recently, an automated technique based on Lunkas–Kanade algorithm was developed to track gastrocnemius aponeurosis and free tendon (Magnusson et al., 2003); and an automated method based on spatial cross correlation for automating the tracking of features frame by frame was developed to track

* Corresponding author.
  E-mail addresses: mrana@sfu.ca, mankurana@gmail.com (M. Rana).

changes in contractile length of muscle fascicles (Loram et al., 2006). This latter method needed an initial manual digitization step to identify the features or fascicles of interest, and then it followed the position of these features over a series of successive frames. The method is most robust when successive frames are most similar, as is the case for low amplitude contractions and small changes in pennation. With substantial changes in pennation angle that occur with large joint movements and muscle contractions, the local features within the ultrasound image change in shape and may even disappear from the ultrasound plane and this can result in error in the measurement.

The purpose of this study was to develop an automated method to quantify the orientation of the fascicles within a muscle from ultrasound images, and to resolve the orientations to localized regions along the fascicles.

2. Methods

2.1. Method overview

B-mode ultrasound images contain information on the muscle fascicle orientation as well as noise. We used a multistage process to determine fascicle orientation (Fig. 1): initial multiscale vessel enhancement filtering enhanced fascicle structure (which is vessel-like or tubular) and decreased the noise level. Fascicle orientation was then determined by two alternate methods: (a) Radon transform was used to quantify the dominant orientation in the image and (b) an ultrasound-specific wavelet analysis quantified the local orientation around each pixel. The two methods were validated against synthetic images with known orientation and also with the real ultrasound images that were additionally digitized manually by 10 people.

2.2. Multiscale vessel enhancement filtering

Muscle fascicles appear dark in the image and connective tissue between the fascicles appears as bright, vessel-like tubular structures that parallel the fascicles. (Frangi et al., (1998) used vesselness filter to enhance muscle fascicles. This method enhances the tubular structures in the image and is capable of resolving tubular structures of different radii and can work with curved tubular structures.

The image was initially convolved with a series of four Gaussian kernels in which each kernel had a normalized Gaussian distribution centered within the kernel. The standard deviations (1.5, 2, 2.5 and 3) for these Gaussian distributions were chosen based on diameter of the tubular structures in the image. If the standard deviation is greater than the diameter there is over-blurring of the image, and if it is lesser it enhances other than picks more noise. The size of the kernel depends on the standard deviations for the kernels that in turn depend on the resolution of ultrasound scanning probe relative to the size of tubular structures in image. In this case we have used 13×13 grids for Gaussian kernels. The Hessian matrix of these convolved images provides second-order information that is related to the vessel direction. For an ideal tubular structure, the Eigenvalues λ_1 and λ_2 of the Hessian matrix obey the following rules:

$$|\lambda_1| \gg |\lambda_2|$$

$$|\lambda_2| = 0$$

The Eigenvector in the direction of the smallest Eigen value represents the local vessel direction. The vesselness response $V(s)$ for each scale was determined as,

$$V(s) = \begin{cases} 0, & \text{if } \lambda_2 > 0 \\ \exp\left(\frac{-R^2}{2\beta^2}\right)\left(1 - \exp\left(\frac{-S}{2c^2}\right)\right), & \text{if } \lambda_2 \leq 0 \end{cases}$$

where $R = |\lambda_1|/|\lambda_2|$ and is a measure of line-like structure; and $S = \sqrt{\sum_{i \leq 2} \lambda_i^2}$ is the Frobenius norm of the Hessian matrix. Period β and c are arbitrary contants both set to 0.5 according to Frangi et al. (1998). The whole process was repeated at each pixel for different scales and the filtered image taken as the maximum vesselness response across the four scales for each pixel (Fig. 2). The figure shown is from relaxed state of the muscle.

2.3. Anisotropic wavelet analysis

Muscle fascicle orientation at each pixel was obtained by using anisotropic wavelet analysis. A wavelet kernel was constructed based on a modified Mortlet wavelet that was extended into 3D and given polarization with a major orientation α (Fig. 3). The kernel was $2k+1$ pixels in both the x and y directions. At any pixel the amplitude of the wavelet $G(x, y)$ was given by:

$$G(x,y) = \exp\left(\frac{x^2 + y^2}{-dk}\right)\cos\left(\frac{2\pi(x\cos\alpha - y\sin\alpha)}{f}\right) + o,$$

where d is the damping of the wavelet, f the spatial frequency and o a linear offset. The spatial frequency should be set to a major frequency of the repeating fascicular structure; this will vary between ultrasound equipment used but can be determined by using the Radon transform on the image where the frequency of the fluctuations of the projection (Fig. 4C) is the same as the spatial frequency of lines in the image. In this study $f = 7$. The damping was set at $d = 2.5622$ to (A) provide decay of the wavelet by the edges of the kernel (with a half-width of $k = 20$) and (B) to satisfy the wavelet condition of zero integral (for $\alpha = 0$ and $o = 0$). However, due to pixilation artifacts, a non-zero value for o must be introduced for non-zero angles α in order to maintain a zero integral. The value for o never exceeded 0.0004% of the maximum value for the wavelet, and so this offset correction made a negligible difference to the results.

The filtered image was convolved with a set of wavelet kernels at different orientations α. The wavelet with orientation α that resulted in the greatest
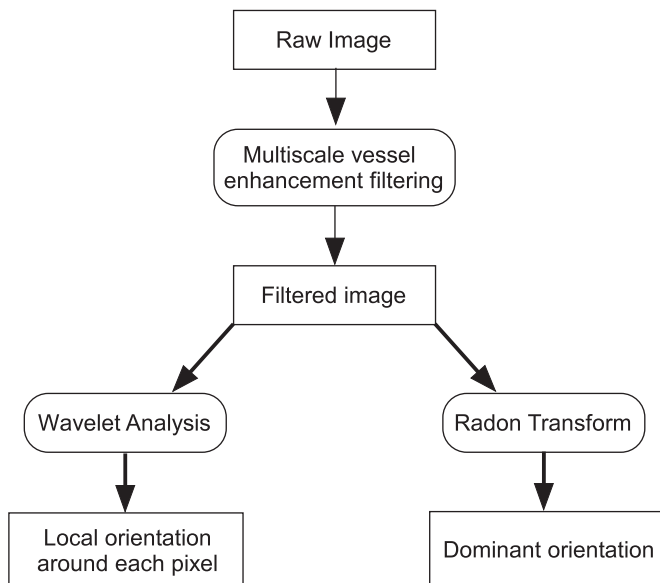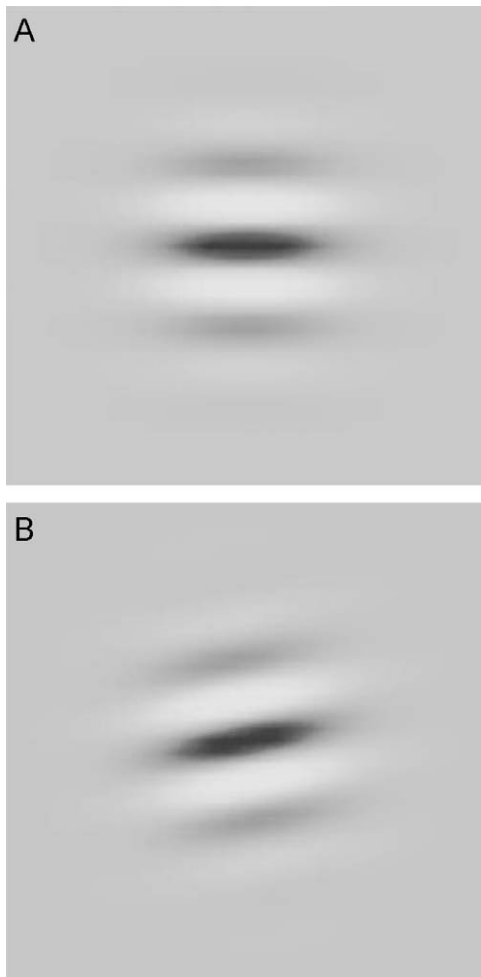
Fig. 2. Ultrasound image from the vastus lateralis (A) and after multi-scale vessel enhancement filtering (B).

Fig. 1. The sequence of methods used to determine fascicle orientation.

Fig. 3. Anisotropic wavelets for identifying fascicle direction within ultrasound images. Wavelets were calculated using Eq. (2), with $d = 2.5622$, $k = 20$, and $f = 7$ and form a 41 by 41 pixel grid. Wavelets are shown for orientation $\alpha = 0°$ (A) and $\alpha = 10°$ (B).

convolution for a given region in the image identified that region as having a muscle fascicle orientation of α. We selected this region as a 160×160 pixels grid with its center in middle of x-axis of image and half the distance between superficial and bottom aponeurosis.

2.4. Radon transform

Radon transforms can be used to determine the predominant orientation in a repeated structure such as the muscle fascicles in an ultrasound image. The Radon transform projects a grid of parallel lines, one pixel apart, across the image and calculates the integral of the image intensities along each line (Khouzani and Zadeh, 2005). The orientation θ of the grid is varied, and when θ approaches the dominant orientation of structures within the image then the Radon transform has greatest variability across the image (Fig. 4): this variability was quantified by its variance or kurtosis. Variance was used for synthetic images, as has been used earlier by Khouzani and Zadeh (2005) and kurtosis was used for real ultrasound images because we found that it worked better for real images than variance. Higher kurtosis indicates that more of the variance is due to infrequent extreme deviations, as opposed to frequent modestly-sized deviations. Since the real images have discontinuous line-like structures at unequal distances relative to each other (as opposed to uniformly distributed continuous lines in the synthetic images) the measure of kurtosis is more sensitive to fascicle orientation in the ultrasound images than the variance. The dominant fascicle orientation was taken as the angle θ at which the Radon transform of the filtered image had the greatest variance (synthetic grids) or kurtosis (ultrasound images).

2.5. Validation

The use of wavelet and Radon transforms for ultrasound images were validated using both synthetic and real images. Synthetic images were grids of parallel lines

at a known orientation that had sinusoidal changes in intensity across (or perpendicular to) the lines, these grids were combined with random noise (Fig. 5). A contrast to noise ratio (CNR) was defined as the ratio of the difference in intensity between bright and dark regions of the image to the sum of noise from those respective regions. For images with distributed pixel intensities the difference in intensity between bright and dark regions was taken as the difference between the mean pixel intensities from the brightest and darkest 50% of the pixels. The noise from each region was quantified by the standard deviation of the image pixels in each region.

$$CNR = \frac{I_{Bright} - I_{Dark}}{\sigma_{Bright} + \sigma_{Dark}}$$

The two methods were tested for synthetic grids at a fixed angle of 10° and different noise levels and then at fixed noise level (CNR = 1.0) but different angles.

To validate the methods against real images, B-mode ultrasound images (Echoblaster, Telemed; LT) were recorded at 45 Hz from the distal part of the left vastus lateralis of a subject during cycling on a stationary ergometer. A linear-array probe (128 elements at 7 MHz) was secured to the skin with elasticated bandages and aligned to a plane in which the muscle fascicles were situated. Bitmap images were extracted for each frame from the ultrasound sequence. The subject provided informed consent for this procedure in accordance with the research ethics procedures at Simon Fraser University. Sixty ultrasound images from the ultrasound sequence were manually digitized by 10 different researchers. Each person digitized the sequence twice, and only the second measurements were used to allow for a training effect in visualizing the fascicles. From each image, a fascicle was identified that spanned from superficial to deep aponeurosis, and two points were digitized on the fascicle close to the aponeurosis. The angle between these points on the fascicle and the x-axis was calculated. A region of interest was identified for each image within the aponeurosis that contained only the muscle fascicles, and this fascicle direction was quantified by the mean α from the wavelet analysis and the dominant orientation θ from the Radon transform (Fig. 6).

3. Results

The images after multiscale vessel enhancement filtering are shown in Fig. 2B. It is clear that this method enhances the fascicle structure in the image and is capable of enhancing fascicles of different diameters. Both the wavelet analysis and Radon transform methods were able to accurately identify the fascicle orientation in the synthetic images (Fig. 7) with a CNR of 0.8. The least squares linear regression for the calculated orientations against the actual orientations for these two methods both had slopes not significantly different from unity (the ideal line). The mean absolute error for the Radon transform across the range 0–90° was 0.058° and the mean error for the wavelet transform across this range was 0.02°. These error values are small enough for practical applications.

When the level of noise increased in the synthetic images there was an increase in the error of the estimate of orientation (Fig. 8). The errors for both the Radon transform and wavelet analysis were less than 0.02° for CNR greater than 0.8. The CNRs for the ultrasound images for the vastus lateralis were in the range 0.85–1.34.

The ultrasound images showed that the fascicle orientations changed in a cyclical fashion during each pedal cycle. The greatest fascicle angles occurred at the bottom of the pedal cycle when the knee was most extended, with a short vastus lateralis length. Manual digitization showed that the mean fascicle angles, relative to the x-axis on each image, varied between 2.0° and 3.5° and this corresponded to pennation angles of 8.6–9.5° that were relative to the deep aponeurosis. Considerable variability occurred in the fascicle orientations that were manually digitized by the 10 researchers (Fig. 9). The standard deviation for the fascicle orientations for each frame had a mean value of 1.41° (range 0.46–2.83°).

The results from the wavelet analysis and Radon transform on the ultrasound images can be visualized in Fig. 6. Lines have been drawn that have an orientation determined from the Radon transform or mean wavelet value, and pass through the center of

A

B

C

D
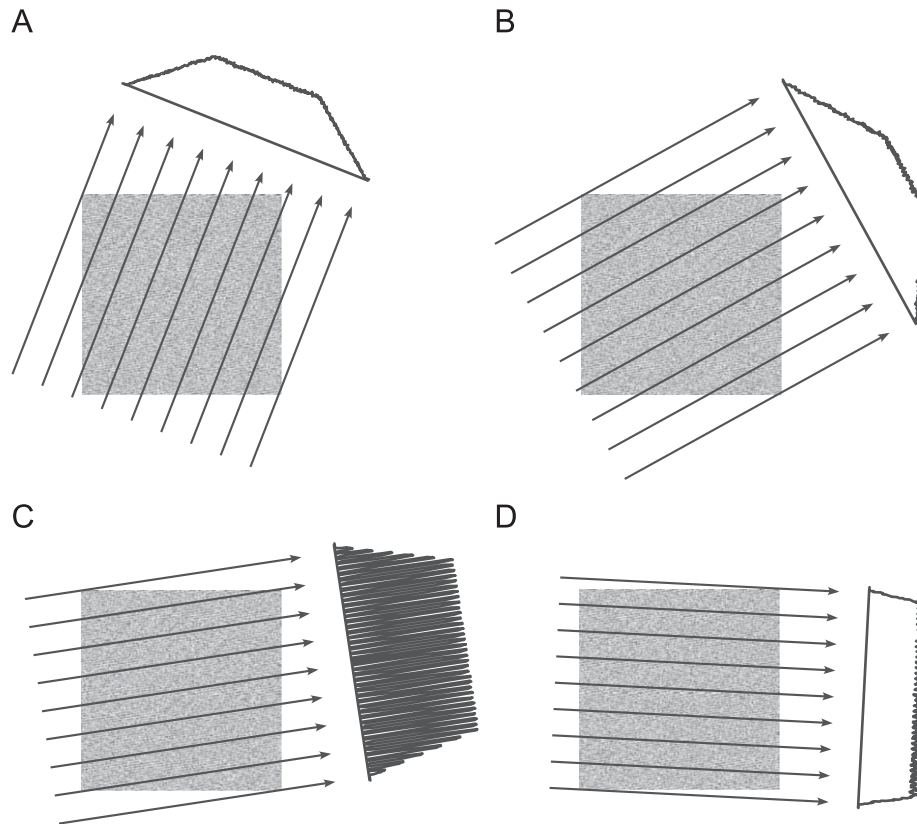
Fig. 4. An illustration of the Radon transform at four different angles θ on a synthetic grid (A–D). The arrows show the projections through the grid. The Radon transform shows the greatest variance when θ approaches the orientation within the grid.

the muscle. In some images the wavelet transform resulted in orientations at lesser angles than for the Radon transform. The mean orientation α from the wavelet analysis was significantly different from the mean fascicle orientation that was manually digitized from each ultrasound frame (two-tailed, matched pair, t-test; $p < 0.001$) with the mean difference being $-1.35°$; this difference was less than the standard deviation of the manually digitized values for each frame of $1.41°$ (Fig. 9). There was no significant difference between the dominant orientation θ from the Radon transform and the manually digitized values from each ultrasound frame (two-tailed, matched pair, t-test; $p = 0.773$).
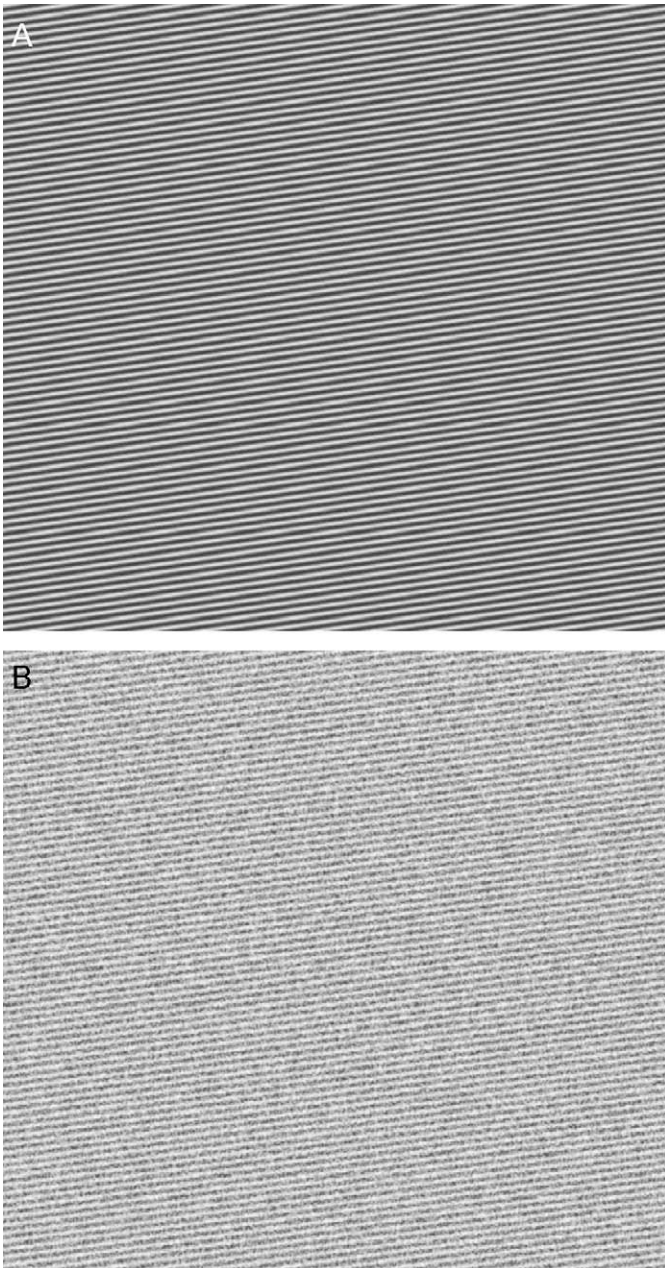
4. Discussion

The combination of multiscale vessel enhancement with either wavelet analysis or Radon transform has resulted in methods that will automatically detect the orientation of fascicular structures within an image. Both methods had accuracy better than $0.02°$ for levels of noise typical of those in ultrasound images (Fig. 8) with the wavelet transform performing slightly better than the Radon transform. When the methods were applied to an actual ultrasound sequence the Radon transform identified orientations with a closer match to the manual values than the wavelet analysis (Fig. 9). This in itself does not show that the wavelet analysis is worse at identifying actual muscle fascicle orientations than the Radon transform because we do not know the accuracy of manually digitizing the sequences, and indeed the different researchers produced a surprising variability in their perceived fascicle directions (standard deviation of $1.41°$). It may be expected that the Radon transform generates similar values to the manually determined ones because it is likely that they follow similar principles. The Radon transform identifies the dominant
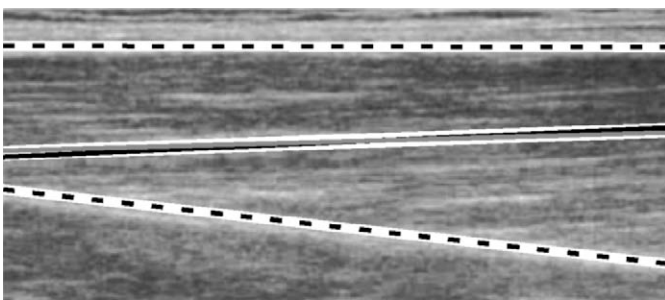
orientation within the image that would correspond to the most prominent and visible fascicles that draw the when being digitized manually. Furthermore, the Radon transform projects parallel straight lines across the image and so would be particularly suitable when identifying linear approximations to the muscle fascicles. These features are particularly useful if the purpose is to identify a "representative" fascicle within the image for determining its linear length, as has been the case for many previous studies.

By contrast, the wavelet transform identifies the mean orientation of the fascicular structures within the space of the kernel. Within the kernel the energy of the wavelet is concentrated within a circular region of radius 11 pixels, corresponding to 1.3 mm in the muscle. Thus the wavelet transform can identify local orientations with a 1.3 mm spatial resolution throughout the ultrasound image. The mean orientations calculated across the image, for validation purposes, contained information about all fascicle orientations within the muscle. Where some fascicles were not in the ultrasound plane, their projected segments in the image would be at different orientations to the fascicles that were in the ultrasound plane; thus, the mean orientations identified by the wavelet analysis would be different from the orientations obtained from fascicles that were visualized as entirely within the scanning plane. Nonetheless, the mean orientations determined from the wavelet analysis were within the range of those manually digitized and thus this method could be used to automatically track whole fascicles for the purposes of determining their linear length.
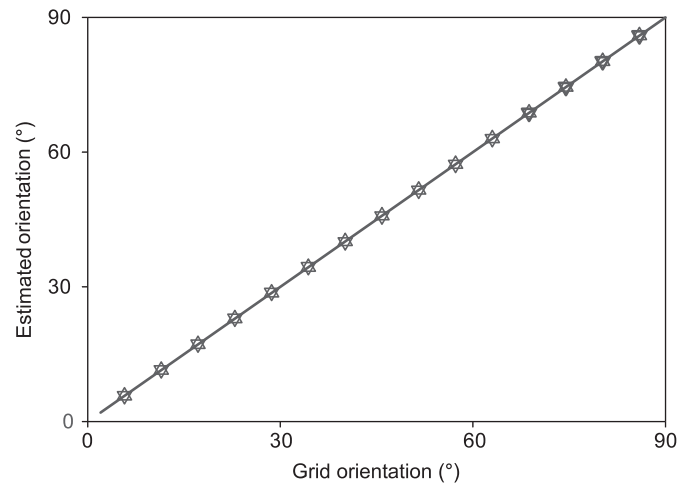
The wavelet transform not only provides the information needed to estimate linear fascicle length, but it additionally resolves the local orientations that can be used to quantify variations in fascicle orientation across an image and variation in orientation along the length of a fascicle such as when the
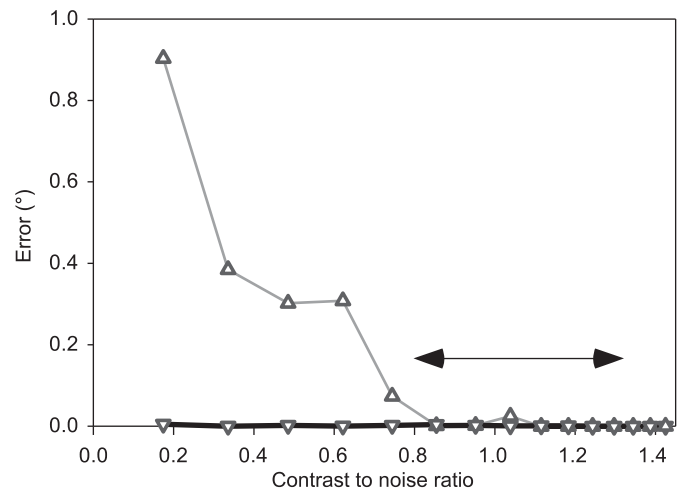
Fig. 7. Estimated orientations from the simulated grids calculated for a range of angles using CNR = 0.75. Angles calculated using the wavelet transform are shown by triangles with apex at top, and angles calculated using the Radon transform are shown by triangles with apex at their bottom. The line shows the ideal result.

Fig. 8. Errors in the estimated orientations from the simulated grids calculated for a range of contrast to noise ratios at a fixed orientation of 8.6°. Angles calculated using the wavelet transform are shown by the grey line and triangles with apex at top, and angles calculated using the Radon transform are shown by the black line and triangles with apex at their bottom. The arrows show the range of contrast to noise ratios observed in ultrasound images from the vastus lateralis.

Fig. 5. Synthetic images used for validations at an orientation of 8.6° with no added noise (A) and with added noise at CNR = 0.79 (B).

Fig. 6. Ultrasound image from the vastus lateralis. The aponeuroses are indicated by the dashed lines. The mean fascicle orientations are shown by the solid black and grey lines from the Radon and wavelet transforms, respectively. Each line is shown against a white relief for clarity.

fascicles are curved. It has been shown that muscle fascicles must follow curved trajectories within a muscle in order to be mechanically stable, particularly for the case of unipennate muscles (van Leeuwen and Spoor, 1992). Fascicle curvatures have previously been determined by manual digitization (Muramatsu et al., 2002), and have been predicted to contribute to the non-uniform strain patterns that are observed along fascicles (Ahn et al., 2003; Pappas et al., 2002; Drost et al., 2003). Fascicle curvature is thus an important aspect of muscle architecture that is commonly overlooked for the ease of assuming and digitizing linear fascicles within a muscle. The combined multiscale vessel enhancement and wavelet analysis methods presented here provide an automatic and objective method for quantifying local fascicle orientations and thus the non-linear trajectories of fascicles through muscles.

Both the wavelet analysis and Radon transform methods assessed in this study can be applied to an image with no prior manual digitization or algorithm training, and they can be applied
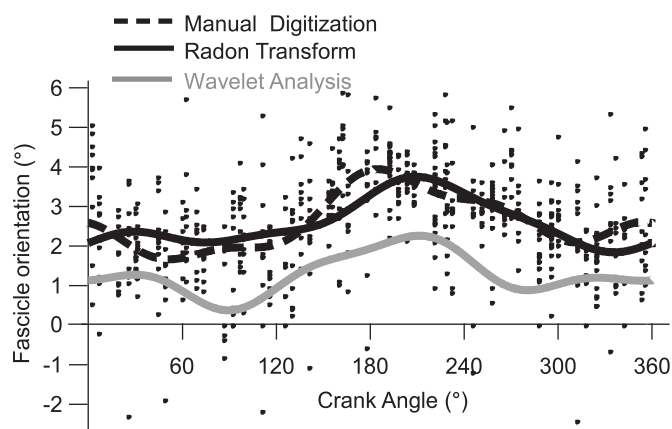
Fig. 9. Muscle fascicle orientations in the vastus lateralis during cycling. Orientations are relative to the ultrasound probe (skin) surface. Points show the orientations determined from manual digitization by 10 researchers. Lines show the orientations determined using Fourier series from the manually digitized points (dashed black line); Radon transform (solid black line) and wavelet transform (solid grey line).

to a single frame as easily as to a sequence. These features represent improvements to previous manual digitization and tracking methods (Loram et al., 2006). The Radon transform can be used to identify the dominant fascicular orientation within an image, and thus used to estimate muscle fascicle lengths. The wavelet analysis additionally provides information on the local fascicle orientations and can be used to quantify fascicle curvatures and regional differences with fascicle orientation across and image.

Conflict of interest

There is no conflict of interest.

Acknowledgements

References

Ahn, A.N., Monti, R.L., Biewener, A.A., 2003. In vivo and in vitro heterogeneity of segment length changes in the toad semimembranosus. J. Physiol. London 549, 877–888.

Azizi, E., Brainerd, E.L., Roberts, T.J., 2008. Variable gearing in pennate muscles. PNAS 105, 1745–1750.

Blazevich, A.J., Gill, N.D., Zhou, S., 2006. Intra- and intermuscular variation in human quadriceps femoris architecture assessed in vivo. J. Anat. 209, 289–310.

Drost, M.R., Maenhout, M., Willems, P.J., Oomens, C.W., Baaijens, F.P., Hesselink, M.K., 2003. Spatial and temporal heterogeneity of superficial muscle strain during in situ fixed-end contractions. J. Biomech. 36, 1055–1063.

Frangi, R.F., Nissen, W.J., Vincken, K.L., Viergever, M.A., 1998. Multiscale vessel enhancement filtering. MICCAI 1496, 130–137.

Fukunaga, T., Ichinose, Y., Ito, M., Kawakami, Y., Fukashiro, S., 1997a. Determination of fascicle length and pennation in a contracting human muscle in vivo. J. Appl. Physiol. 82 (1), 354–358.

Fukunaga, T., Kawakami, Y., Kuni, S., Funato, K., Fukashiro, S., 1997b. Muscle architecture and function in humans. J. Biomech. 30, 457–463.

Herbert, R.D., Gandevia, S.C., 1995. Changes in pennation with joint angle and muscle torque *in vivo* measurements in human brachialis muscle. J. Physiol. 484, 523–532.

Ichinose, Y., Kawakami, Y., Ito, M., Kaneshia, H., Fukunga, T., 2000. In vivo estimation of contraction velocity of human vastus lateralis muscle during "isokinetic" contraction. J. Appl. Physiol. 88, 851–856.

Ishikawa, M., Finni, T., Komi, P.V., 2003. Behaviour of vastus lateralis muscle during high intensity SSC exercise in vivo. Acta Physiol. Scand. 178, 205–213.

Ito, M., Kawakami, Y., Ichinose, Y., Fukashiro, S., Fukunga, Y., 1998. Nonisometric behavior of fascicles during isometric contractions of human muscles. J. Appl. Physiol. 85 (4), 1230–1235.

Kawakami, Y., Abe, T., Fukunaga, T., 1998. Muscle–fiber pennation angles are greater in hypertrophied than in normal muscles. J. Appl. Physiol. 74, 2740–2744.

Kawakami, Y., Muraoka, T., Ito, S., Kanehisa, H., Fukunaga, T., 2002. In vivo muscle fibre behaviour during counter movement exercise in humans reveals a significant role for tendon elasticity. J. Physiol. 540, 635–646.

Khouzani, K.J., Zadeh, H.A., 2005. Radon transform orientation estimation for rotation invariant texture analysis. IEEE 27, 1004–1008.

Kurokawa, S., Fukunaga, T., Fukashiro, S., 2001. Behavior of fascicles and tendinous structures of human gastrocnemius during vertical jumping. J. Appl. Physiol. 80, 1349–1358.

Kurokawa, S., Fukunaga, T., Nagano, A., Fukashiro, S., 2003. Interaction between fascicles and tendinous structures during counter movement jumping investigated in vivo. J. Appl. Physiol. 95, 2306–2314.

Lieber, R.L., Fridén, J., 2000. Functional and clinical significance of skeletal muscle architecture. Muscle Nerve 11, 1647–1666.

Loram, I.D., Maganaris, C.N., Lakie, M., 2006. Use of ultrasound to make noninvasive in vivo measurement of continuous changes in human muscle contractile length. J. Appl. Physiol. 100, 1311–1323.

Maganaris, C.N., Baltzopoulos, V., Sargeant, A.J., 1998. In vivo measurements of the triceps surae complex architecture in man: implications for muscle function. J. Physiol. 512, 603–614.

Magnusson, S.P., Hansen, P., Aagaard, P., Brond, J., Dyhre-Polsen, P., Bojsen-Moller, J., Kjare, M., 2003. Differential strain patterns of human gastrocnemius aponeurosis and free tendon, in vivo. Acta Physiol. Scand. 177, 185–195.

Muramatsu, T., Tetsuro, M., Kawakami, Y., Shibayama, A., Fukunaga, T., 2002. In vivo determination of fascicle curvature in contracting human skeletal muscles. J. Appl. Physiol. 92, 129–134.

Muraoka, T., Kawakami, Y., Tachi, M., Funkunga, T., 2001. Muscle fiber and tendon length changes in the human vastus lateralis during slow pedaling. J. Appl. Physiol. 91, 2035–2040.

Narici, M.V., Binzoni, T., Hiltbrand, E., Fasel, J., Terrier, F., Cerretelli, P., 1996. In vivo human gastrocnemius architecture with changing joint angle at rest and during graded isometric contraction. J. Physiol. 496, 287–297.

Pappas, G.P., Asakawa, D., Delp, S.L., Zajac, F.E., Drace, J.E., 2002. Nonuniform shortening in the biceps brachii during elbow flexion. J. Appl. Physiol. 92, 2381–2389.

Van Leeuwen, J.L., Spoor, C.W., 1992. Modeling mechanically stable muscle architectures. Phil. Trans. R. Soc. London B Biol. Sci. 336 (1277), 275–292.

Wakeling, J.M., Uehli, K., Rozitis, A.I., 2006. Muscle fibre recruitment can respond to the mechanics of the muscle contraction. J. R. Soc. Interface 3, 533–544.